Different domains in nidogen-1 and nidogen-2 drive basement membrane formation in skin organotypic cocultures

Manuela Bechtel,* Manuel V. Keller,† Wilhelm Bloch,‡ Takako Sasaki,§ Petra Boukamp,‖ Frank Zaucke,†,¶,# Mats Paulsson,† and Roswitha Nischt*,[1]

*Department of Dermatology, University Hospital of Cologne, Cologne, Germany; †Center for Biochemistry, Medical Faculty, ¶Center for Molecular Medicine Cologne, and #Cologne Excellence Cluster on Cellular Stress Responses in Aging-Associated Diseases, University of Cologne, Cologne, Germany; ‡Department of Molecular and Cellular Sport Medicine, Institute of Cardiology and Sport Medicine, German Sport University Cologne, Cologne, Germany; §Department of Experimental Medicine I, Nikolaus-Fiebiger Center of Molecular Medicine, University of Erlangen-Nürnberg, Erlangen, Germany; and ‖German Cancer Research Center, Division of Genetics of Skin Carcinogenesis, Heidelberg, Germany

ABSTRACT **Nidogen-1 and nidogen-2 are homologous proteins found in all basement membranes (BMs). They show comparable binding activities *in vitro* and partially redundant functions *in vivo*. Previously, we showed that in skin organotypic cocultures, BM formation was prevented in the absence of nidogens and that either nidogen was able to rescue this failure. We now dissected the two nidogens to identify the domains required for BM deposition. For that purpose, HaCaT cells were grown on collagen matrices containing nidogen-deficient, murine fibroblasts. After addition of nidogen-1 or nidogen-2 protein fragments comprising different binding domains, BM deposition was analyzed by immunofluorescence and electron microscopy. We could demonstrate that the rod-G3 domain of nidogen-2 was sufficient to achieve deposition of BM components at the epidermal-collagen interface. In contrast, for nidogen-1, both the G2 and G3 domains were required. Immunoblot analysis confirmed that all BM components were present in comparable amounts under all culture conditions. This finding demonstrates that nidogens, although homologous proteins, exert their effect on BM assembly through different binding domains, which may in turn result in alterations of BM structure and functions, thus providing an explanation for the phenotypical differences observed between nidogen-1 and -2 deficient mice.—Bechtel, M., Keller, M. V., Bloch, W., Sasaki, T., Boukamp, P., Zaucke, F., Paulsson, M., Nischt, R. Different domains in nidogen-1 and nidogen-2 drive basement membrane formation in skin organotypic cocultures. *FASEB J.* 26, 3637–3648 (2012). www.fasebj.org**

Key Words: 3-dimensional coculture system · laminin-collagen connecting activity

Basement membranes (BMs) are highly specialized extracellular matrices underlying all epithelia and endothelia as well as enveloping several mesenchymal cell types. All BMs contain at least one representative of each of the laminin, nidogen, collagen IV, and proteoglycan families (1–3). Both laminin and collagen IV molecules form *in vitro* networks by self-assembly. *In vivo* the initial development of BMs requires the presence of laminins (3, 4), whereas mechanical strength seems to be largely implemented by collagen IV (5).

The mammalian nidogen family consists of two members, nidogen-1 and nidogen-2. Both are ubiquitous BM proteins with a similar distribution in various organs during development. However, in adult tissues nidogen-2 distribution becomes more restricted (6–8). Both nidogens have a wide spectrum of interaction partners, in particular, the other main BM components laminin, collagen IV, and perlecan (6, 8–10). Through these interactions they are assumed to connect and stabilize the major networks formed by laminin and collagen IV and target mesenchymal nidogen to the epithelial as well as endothelial BMs (6, 9, 11). Nidogen-1 and -2 share a modular structure with 3 globular domains, G1, G2, and G3, separated by a link region between G1 and G2 and by a rod-like region between G2 and G3 (**Fig. 1*A*** and **Table 1**). Nidogen-1, a 150-kDa protein, is somewhat shorter (30 nm) than the 200-kDa nidogen-2 (40–45 nm) (6, 8, 9).

Abbreviations: 3D, 3-dimensional; BM, basement membrane; EGF, epidermal growth factor; LDLR, LDL receptor

[1] Correspondence: Department of Dermatology, University Hospital of Cologne, KerpenerStraße 62, D-50937 Cologne, Germany. E-mail: roswitha.nischt@uni-koeln.de

doi: 10.1096/fj.11-194597

This article includes supplemental data. Please visit *http://www.fasebj.org* to obtain this information.

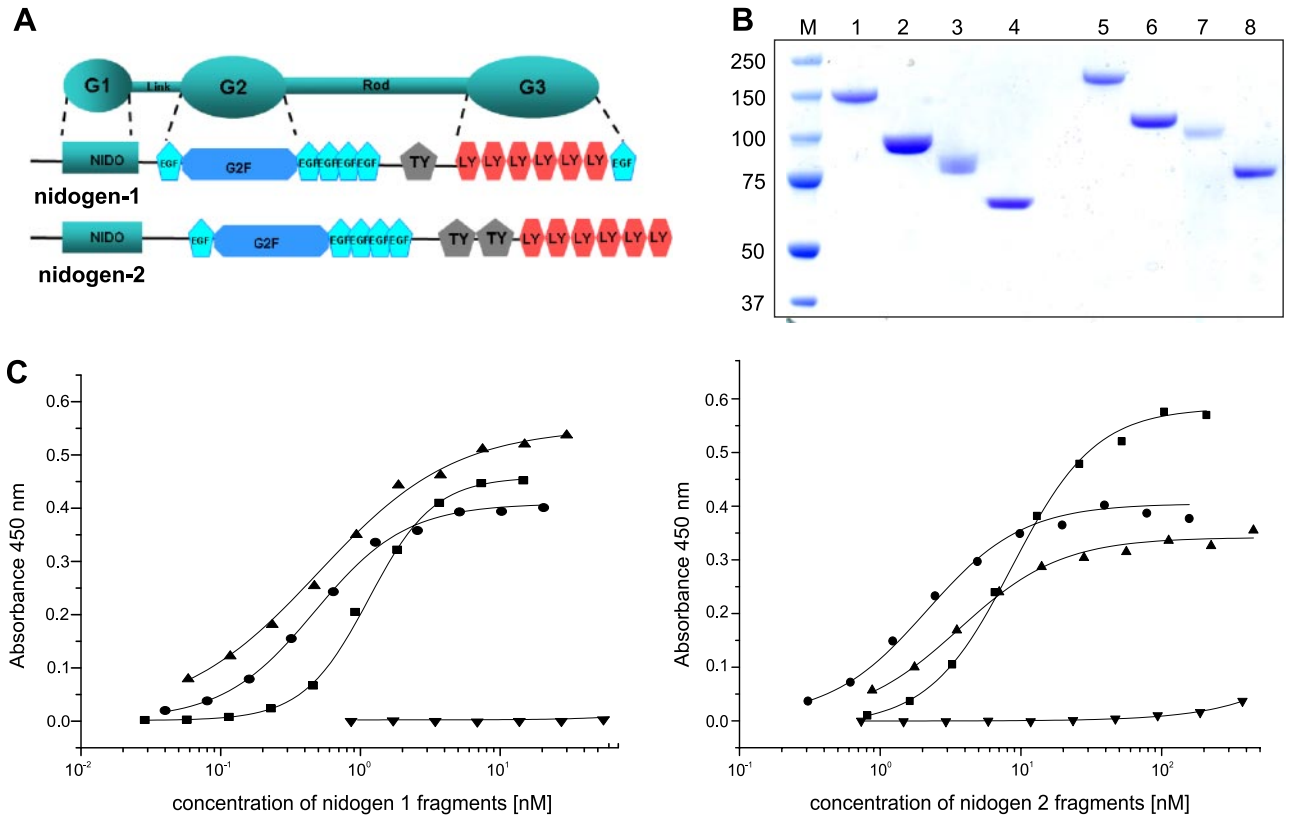

Figure 1. Boundaries and properties of recombinant nidogen fragments. *A*) Schematic diagram of the modular nidogen structure with the globular domains G1, G2, G3, the link region, and the rod domain and detailed domain structures of nidogen-1 and nidogen-2. See Table 1 for sequence position and molecular mass of fragments. Nido, nidogen-like domain; G2F, G2 nidogen and fibulin module; EGF, epidermal growth factor-like module; TY, thyroglobulin type-1 module; LY, low density lipoprotein receptor YWTD repeat. *B*) SDS-PAGE of purified recombinant nidogen fragments. Lanes were loaded with 2 μg of nidogen-1 (lane 1), nidogen-1 G2–G3 (lane 2), nidogen-1 G1–G2 (lane 3), nidogen-1 rod–G3 (lane 4), nidogen-2 (lane 5), nidogen-2 G2–G3 (lane 6), nidogen-2 G1–G2 (lane 7), and nidogen-2 rod–G3 (lane 8). All proteins were reduced before electrophoresis. Calibration with reduced standard proteins (*M*) is shown at left. Proteins were stained with Coomassie Brilliant Blue R-250. *C*) Binding activities of recombinant mouse nidogen-1 (left panel) and nidogen-2 (right panel) and their fragments in solid-phase binding assays. The short arm of the laminin γ1 chain was used as the immobilized ligand. Soluble ligands used were full-length mouse nidogen-1 and -2 (■) and fragments comprising G2–G3 (●), G1–G2 (▼), and rod–G3 (▲) domains. Bound ligands were detected with a mouse monoclonal antibody against the His tag, followed by incubation with a horseradish peroxidase-conjugated secondary antibody and tetramethylbenzidine as substrate. Absorption was measured at 450 nm.

The G3 domain of nidogen-1 has been shown to bind with high affinity to the γ1III4 module located on the laminin γ1 short arm (9, 12–14). The binding surface for collagen IV was localized to the G2 domain of nidogen-1, which also carries the perlecan interaction site (9, 11, 14). On the basis of structural similarities and comparable binding activities of full-length nidogen-1 and -2, it is assumed that nidogen-2 binds to collagen IV and laminin *via* the same domains as nidogen-1 (6, 8).

TABLE 1. *Boundaries and properties of recombinant nidogen fragments*

Domain	Sequence position	Molecular mass (kDa)
Nidogen-1	29–1245	154
Nidogen-1 G2–G3	385–1245	109
Nidogen-1 G1–G2	29–666	95
Nidogen-1 rod–G3	666–1245	71
Nidogen-2	31–1403	178
Nidogen-2 G2–G3	507–1403	131
Nidogen-2 G1–G2	31–784	121
Nidogen-2 rod–G3	785–1403	89

Numbering of amino acid residues does not include the signal peptide. Molecular masses are those determined by SDS-PAGE under reducing conditions.

Although nidogen-1 and nidogen-2 display redundant functions, phenotypical differences between mice lacking either nidogen-1 or -2 have been observed (7, 15, 16). Nidogen-1-deficient mice show wound healing defects and neurological abnormalities not seen in the absence of nidogen-2 (17, 18). Furthermore, analysis of mice lacking the nidogen-binding module on the laminin γ1 chain revealed that only nidogen-1 is lost from BMs in the absence of this module, whereas nidogen-2 is still retained (19, 20). This demonstrates that nidogen-2 is independently recruited either by binding to an alternative site on laminin or to other BM proteins. Interestingly, although the BM structure appeared ultrastructurally normal, these mice showed

epidermal thickening and hyperproliferation (20). These results demonstrate that *in vivo* nidogen-1 and -2 have partially different functions which may be attributed to differences in their binding behavior.

Skin organotypic 3-dimensional (3D) cocultures reflect many features of human or mouse skin. In this model a BM is formed between keratinocytes growing at the air-liquid interface and a collagen gel populated with dermal fibroblasts (21–25). Using dermal fibroblasts isolated from mice lacking expression of both nidogen isoforms (16) together with HaCaT cells (26–28), we showed previously that complete nidogen deficiency led to the loss of all major BM components from the epidermal-collagen gel interface. At the ultrastructural level, a defined BM zone was completely missing, and hemidesmosomes failed to develop (29). The addition of either recombinant nidogen-1 or nidogen-2 to the culture medium compensated for these defects, making the system ideally suited to determine whether nidogen-1 or -2 rescues these defects through the same binding domains.

In the current study, we demonstrate that nidogen-1 and -2 use different binding domains to trigger deposition of BM components at the epidermal-collagen interface in a skin organotypic coculture system.

MATERIALS AND METHODS

Preparation of expression vectors and transfected cells

Full-length cDNAs encoding mouse nidogen-1 in pBluescript (9) or nidogen-2 in a pUC19 vector (8) were used as templates for the amplification of individual fragments by PCR with Phusion High-Fidelity polymerase (New England Biolabs, Frankfurt, Germany) following the manufacturer's protocol. The oligonucleotide primers used for the 5′ and 3′ ends were the following: for nidogen-1 domain G1−G2, 5′-TTTGCTAGCTCTGAATCGCCAGGAGCTCTTC-3′ and 5′-TTTGCGGCCGCAAGGGCATCAGGGGAGCCAT-3′; domain G2−G3, 5′-TTTGCTAGCTCAGCAGACTTGTGCCAACAA-3′ and 5′-TTTGCGGCCGCTTTCCGTTCAATGCAGTCAACTC-3′; and domain rod−G3, 5′-TTTGCTAGCTCTTCAGAATCCATGCTACATTGG-3′ and 5′-TTTGCGGCCGCTTTCCGTTCAATGCAGTCAACTC-3′; and for nidogen-2 domain G1−G2, 5′-TTTGCTAGCTCTGCGTCCCGACGAGCTCTT-3′ and 5′-TTTGCGGCCGCATTCACTCCAACAGGGGCTGAGT-3′; domain G2−G3, 5′-TTTGCTAGCTAACCTGGAAACCTGCGAACACA-3′ and 5′-TTTGCGGCCGCTTTTCTTCCTGTTGGACAGTACGG-3′; and domain rod−G3, 5′-TTTGCTAGCTCCTTGCTACGACGGAAGCCA-3′ and 5′-TTTGCGGCCGCTTTTCTTCCTGTTGGACAGTACGG-3′. The primers were designed to introduce a *Nhe*I site at the 5′ end and a *Not*I site at the 3′ end to ligate the amplified cDNA in frame to the BM-40 signal peptide sequence into a modified pCEP-Pu vector carrying a His_6-tag (30). For the short arm of the mouse laminin γ1 chain (aa 34-1128, molecular mass 113 kDa) the primer pair 5′-TTAGCTAGCAGCCATGGACGAGTGCGCGGATG-3′ and 5′-TTTCTCGAGCTCCTGGCAGCCAGGCCAGGAC-3′ was used. The primers were designed to introduce a *Nhe*I site at the 5′ end and an *Xho*I site at the 3′ end to ligate the amplified cDNA in frame to the BM-40 signal peptide sequence of a modified pCEP-Pu expression vector carrying at the 3′ end a thrombin cleavage site followed by two streptavidin tags and one FLAG tag (C-Strep/FLAG-pCEP-Pu). This plasmid was kindly provided by M. Koch (Center for Biochemistry and Center for Dental Medicine, Medical Faculty, University of Cologne, Cologne, Germany).

These episomal expression vectors were used to transfect 293-EBNA human kidney cells using the FuGene 6 transfection reagent (Roche Diagnostics, Mannheim, Germany) followed by selection with puromycin. Cells transfected with mouse full-length nidogen-1 and -2 cDNAs were kindly provided by N. Smyth (School of Biological Sciences, University of Southampton, Southampton, UK). The expression levels of recombinant proteins were examined by SDS-PAGE of serum-free culture medium.

Purification of recombinant proteins

Serum-free conditioned medium was supplemented with 0.5 μM PMSF and passed over a gelatin-Sepharose 4B precolumn followed by Ni Sepharose 6 Fast Flow (GE Healthcare, Munich, Germany), both equilibrated in 0.02 M Tris/HCl (pH 8.0) and 0.15 M NaCl. The elution was performed with a gradient of imidazole (5–250 mM). To remove imidazole, the protein-containing fractions were dialyzed against TBS (pH 8.0). Medium containing the short arm of the laminin γ1 chain was passed over a streptavidin-Sepharose column (GE Healthcare) equilibrated with 0.02 M Tris/HCl (pH 7.5) and 0.15 M NaCl and eluted with 2.5 mM desthiobiotin in PBS. Collagen IV was derived from pepsin digests of human placenta (Sigma-Aldrich, Munich, Germany).

Solid-phase binding assays

The purified short arm of the laminin γ1 chain or collagen IV was coated at 500 ng/well overnight at 4°C onto 96-well plates. After washing with TBS/0.05% Tween 20, plates were blocked for 2 h at room temperature with TBS/1% BSA. Different His-tagged nidogen fragments used as soluble ligands were diluted to concentrations between 0.1 and 500 nM and incubated with the immobilized ligands for 1 h at room temperature. Bound ligands were detected with a mouse monoclonal anti-His antibody. For detection of ternary complex formation, the His-tagged nidogen fragments were preincubated with the streptavidin-tagged short arm of the laminin γ1 chain in a 1:2 molar ratio for 2 h at room temperature. This mixture was then added to the wells coated with collagen IV as described above. After repeated washing with TBS/0.05% Tween 20, bound ligands were detected either with a mouse monoclonal anti-His antibody (1:1000; Qiagen, Hilden, Germany) or a mouse monoclonal anti-streptavidin antibody (1:500; Qiagen) followed by incubation with a horseradish peroxidase-conjugated secondary antibody (1:1000; Dako, Hamburg, Germany) and tetramethylbenzidine as substrate. Absorption was measured at 450 nm after the reaction was stopped with 10% sulfuric acid. All binding assays were performed in duplicate in ≥2 independent experiments.

Skin organotypic 3D coculture

The 3D coculture system applied in this study was described previously (26). In brief, HaCaT cells (1×10^6 cells/cm^2) were grown submersed on collagen I gels populated with mouse skin fibroblasts (2×10^5 cells/ml) lacking expression of both nidogen isoforms, using 25-mm filter inserts. The cocultures were placed in 6-well plates. After 1 d, they were exposed to the air-liquid interface. Treatment of the cocultures with different nidogen-1 or nidogen-2 domains (3 μg/ml each)

was started after 3 d by adding new protein every second day to the cell culture medium throughout the cultivation time. Fibroblasts were prepared from newborn mouse skin. In brief, the skin was removed and after several washes with PBS was floated on 0.25% trypsin (in PBS) at 4°C, epidermal side up. The next day the dermis was separated from the epidermis, minced, and treated with 400 U/ml collagenase type I (Worthington, St. Katharinen, Germany) for 1–2 h at 37°C. After vigorous pipetting, cells were collected by centrifugation at 210 *g* for 5 min and resuspended in DMEM (Life Technologies, Darmstadt, Germany). Fibroblasts were seeded and cultured in DMEM with 10% FCS (PAA, Cölbe, Germany), supplemented with 2 mM glutamine, 100 U/ml penicillin, and 100 μg/ml streptomycin (all from Biochrom, Berlin, Germany) and 50 μg/ml ascorbate (Sigma-Aldrich) at 5% CO_2 and 37°C. Nearly confluent fibroblasts were subcultured by trypsinization. HaCaT cells were grown as described (29). Each set of 3D cocultures (nidogen-1+fragments or nidogen-2+fragments) was repeated 3 times, each time using skin fibroblasts isolated from a different newborn nidogen double-null mouse.

Indirect immunofluorescence and immunoblot analysis

3D coculture samples were fixed in 4% paraformaldehyde in PBS on ice for 60 min. After that they were placed in 1% agar and fixed for additional 2 h. For immunofluorescence analysis, samples were snap-frozen in optimal cutting temperature compound (O.C.T. Tissue Tec; Sakura Finetek Europe, Zoeterwoude, The Netherlands). Cryosections were fixed for 10 min with ice-cold ethanol, blocked for 1 h in 10% normal goat serum, and incubated with primary antibodies for 1 h and with secondary antibodies for 45 min at room temperature. Rabbit polyclonal antibodies raised against the following antigens were used: laminin γ1 chain (kindly provided by N. Smyth, School of Biological Sciences, University of Southampton, Southampton, UK), laminin α5 chain (kindly provided by L. Sorokin, Institute of Physiological Chemistry and Pathobiochemistry, Westfälische Wilhelms-Universität Münster, Münster, Germany), laminin-332 (kindly provided by M. Aumailley, Biochemistry II, University of Cologne, Cologne, Germany), nidogen-1, nidogen-2, and perlecan, keratin 10 (Covance Babco, Richmond, CA, USA), and collagen IV (Biozol, Eching, Germany). The guinea pig polyclonal antibodies against keratin 14 were from Progen (Heidelberg, Germany), and rat monoclonal antibodies raised against the integrin α6 chain were from Abcam (Cambridge, UK). The appropriate secondary antibodies conjugated to Alexa 488 (green) or Alexa 594 (red) (Molecular Probes, Life Technologies, Darmstadt, Germany) were applied together with propidium iodide or DAPI for counterstaining the nuclei. Sections were embedded in mounting media. Immunostaining was examined with an Olympus IX71 Delta Vision microscope (Olympus, Tokyo, Japan).

For immunoblot analysis, the cocultures were homogenized in 200 μl of RIPA extraction buffer (150 mM NaCl, 0.1% Triton X-100, 0.1% SDS, 0.1% deoxycholate, 5 mM EDTA, and 10 mM Tris-HCl, pH 7.2) and a protease inhibitor cocktail (Roche Diagnostic, Mannheim, Germany). Samples were incubated on ice for 1 h and cleared by centrifugation. Then 50 μg of total protein per lane was separated on 4–12% SDS-polyacrylamide gradient gels under reducing conditions. After transfer, the membranes were incubated with primary antibodies, and reactive bands were detected with the appropriate horseradish peroxidase-conjugated secondary antibodies (Dako), followed by chemiluminescence (ECL; GE Healthcare). Equal protein loading was assessed by applying a rabbit polyclonal antibody raised against GAPDH (1:6000; Sigma-Aldrich). In addition to the antibodies listed above, rabbit polyclonal antibodies raised against the laminin γ1 chain (H-190) and goat polyclonal antibodies raised against the laminin γ2 chain (C-20) were used (Santa Cruz Biotechnology, Santa Cruz, CA, USA).

Electron microscopy

Specimens were fixed in 2% paraformaldehyde and 2% glutaraldehyde (in cacodylate buffer, pH 7.4) followed by 2% osmium tetroxide, rinsed 3 times in cacodylate buffer, and then treated with 1% uranyl acetate in 70% ethanol for 8 h to enhance the contrast. The specimens were subsequently dehydrated in a graded series of ethanol and embedded in Araldite (Serva, Heidelberg, Germany). Ultrathin sections (30–60 nm) were cut with a diamond knife on an ultramicrotome and placed on copper grids. Transmission electron microscopy was performed using a Zeiss 902A electron microscope (Carl Zeiss, Oberkochen, Germany).

RESULTS

Recombinant production of nidogen-1 and nidogen-2 fragments

Episomal expression vectors encoding different parts of nidogen-1 and nidogen-2 (Fig. 1*A* and Table 1)were used to produce His-tagged proteins in human 293-EBNA cells and to purify them from serum-free culture medium by chromatography on nickel-loaded columns. The nidogen-1 or -2 fragment G1–G2 comprises the two globular domains G1 and G2 connected by the linker region, the fragment G2–G3 comprises the two globular domains G2 and G3 connected by the rod domain, and the fragment rod–G3 comprises the rod and G3 domain. Addition of the rod improves expression of G3, whereas no binding activities have been assigned to the rod domain (14). SDS-PAGE analysis of the purified fragments under reducing conditions showed for all fragments a single major band (Fig. 1*B*) with the molecular masses given in Table 1.

In both nidogen-1 and nidogen-2 the G3 domain carries the laminin binding site

Previous binding studies performed in solid-phase assays showed that mouse nidogen-1 and nidogen-2 interact with comparable affinities with the laminin fragment P1, which contains the γ1 chain module γ1III4 responsible for high-affinity interaction (8, 12). In nidogen-1, the C-terminal globule G3 has been identified as the laminin-binding domain (9). For nidogen-2, the laminin binding site has not been determined. We therefore tested the different nidogen fragments for their laminin-binding activity in solid-phase binding assays using the short arm of the laminin γ1 chain as the immobilized ligand. Only nidogen-1 and -2 fragments containing the G3 domain, namely the full-length protein and the fragments G2–G3 and rod–G3, bound to the laminin fragment (Fig. 1*C*). The domains G1–G2 of both nidogen-1 and -2 showed no binding activity. This result identifies the G3 domain of nido-

gen-2 as the laminin binding site, as shown before for nidogen-1 (9, 14).

In contrast to nidogen-1, nidogen-2 requires only the G3 domain to rescue BM deposition and formation in skin organotypic cocultures

Previously we showed that in 3D cocultures composed of HaCaT cells and collagen gels populated with nidogen-deficient fibroblasts, deposition of the BM components laminin and collagen IV was prevented (29). As shown in Supplemental Fig. S1, fibroblasts are the only source for nidogens in this coculture system. Addition of recombinant nidogen-1 or nidogen-2 could restore deposition of these proteins at the epidermal interface (**Figs. 2*I, J, M, N*** and **3*I, J, M, N***) (29). To identify the nidogen domains required to rescue BM formation, the cocultures were supplemented with different nidogen fragments throughout the cultivation time. After 12 d, the cocultures were harvested and analyzed by immunofluorescence and electron microscopy.

We first analyzed whether supplementation of the cocultures with nidogen fragments interferes with epithelial organization and differentiation. Immunofluorescence with antibodies against keratin 14 (marker for basal keratinocytes) and keratin 10 (early differentiation marker) revealed no significant differences in protein localization and staining intensities between cocultures without nidogens and cocultures supplemented with nidogen-1 or -2 fragments (Figs. 2*A–D* and 3*A–D*). Further, under all culture conditions the integrin α6 chain (part of the hemidesmosomal integrin α6β4) mainly decorated the junctional interface in a linear fashion, indicating normal epithelial organization (Figs. 2*E–H* and 3*E–H*).

Analysis of 3D cocultures supplemented with nidogen-1 and its fragments revealed that only the full-length nidogen-1 was able to trigger deposition of both the laminin γ1 chain (part of the main isoform laminin-511) and collagen IV at the epidermal-collagen gel interface (Fig. 2*J, N*), whereas the domains G1–G2 (Fig. 2*K, O*) and rod–G3 (Fig. 2*L, P*) were unable to do so. With the domain G1–G2, some patchy collagen IV deposition could be detected (Fig. 2*O*). In contrast, cocultures supplemented with nidogen-2 and its fragments showed that in addition to nidogen-2, the rod-G3

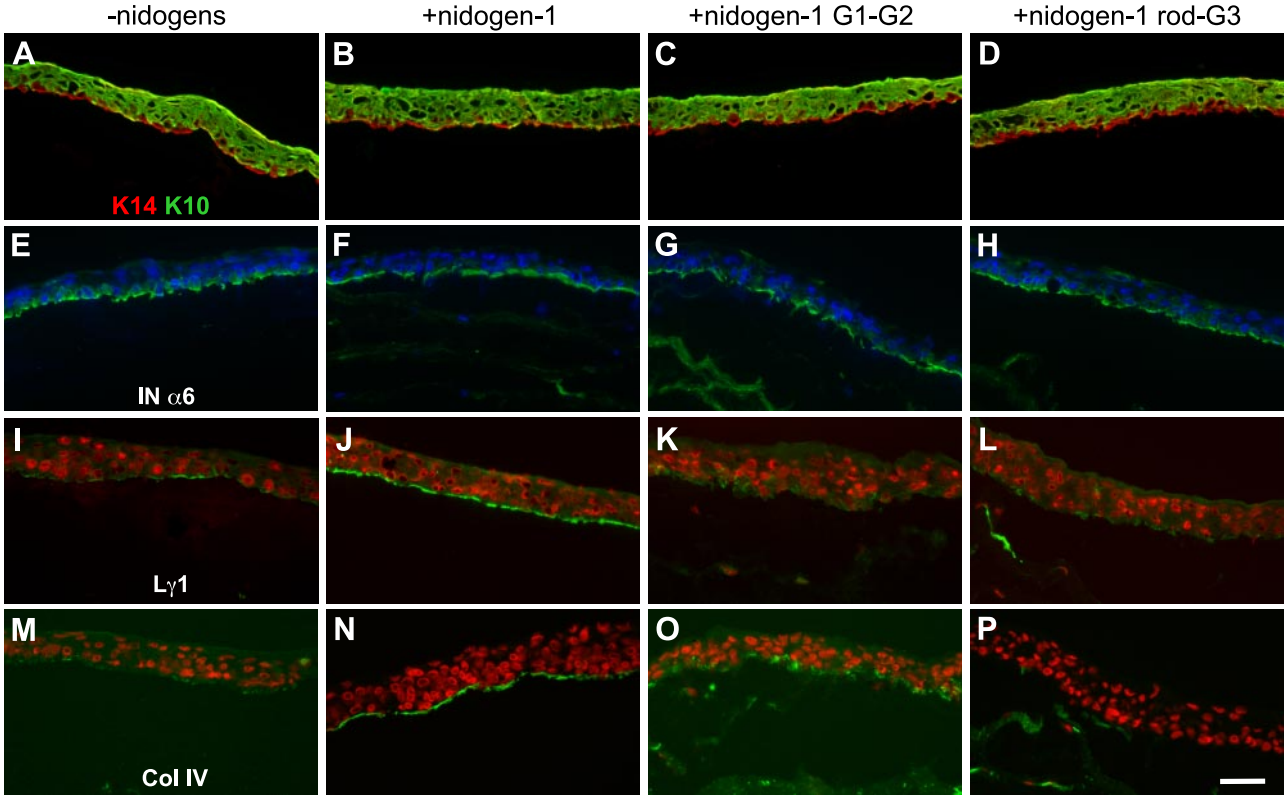

Figure 2. Epithelial organization and deposition of BM components in 3D cocultures. Images show immunofluorescence stainings of cryosections from cocultures with nidogen-deficient mouse fibroblasts without (*A, E, I, M*) and with addition of either 3 μg/ml recombinant nidogen-1 (*B, F, J, N*), nidogen-1 G1–G2 (*C, G, K, O*), or nidogen-1 rod-G3 (*D, H, L, P*) to the culture medium. Supplementation was performed throughout the cultivation time of 12 d. Epithelial organization and onset of differentiation were assessed by immunofluorescence staining for the basal keratin 14 (K14; *A–D*), the suprabasal keratin 10 (K10; *A–D*), and the integrin α6 chain (IN α6; *E–H*). Deposition of BM components was analyzed using antibodies raised against the laminin γ1 chain (Lγ1; *I–L*), detecting laminin-511, and collagen IV (Col IV; *M–P*). Secondary antibodies conjugated to Alexa 488 (green) were used to detect the integrin α6 chain, the laminin γ1 chain, collagen IV, and keratin 10, and Alexa 594 (red) was used to detect keratin 14. Propidium iodide (red) or DAPI (blue) was used to stain nuclei. A representative set of cocultures out of 3 independently performed experiments is shown. Scale bar = 40 μm.

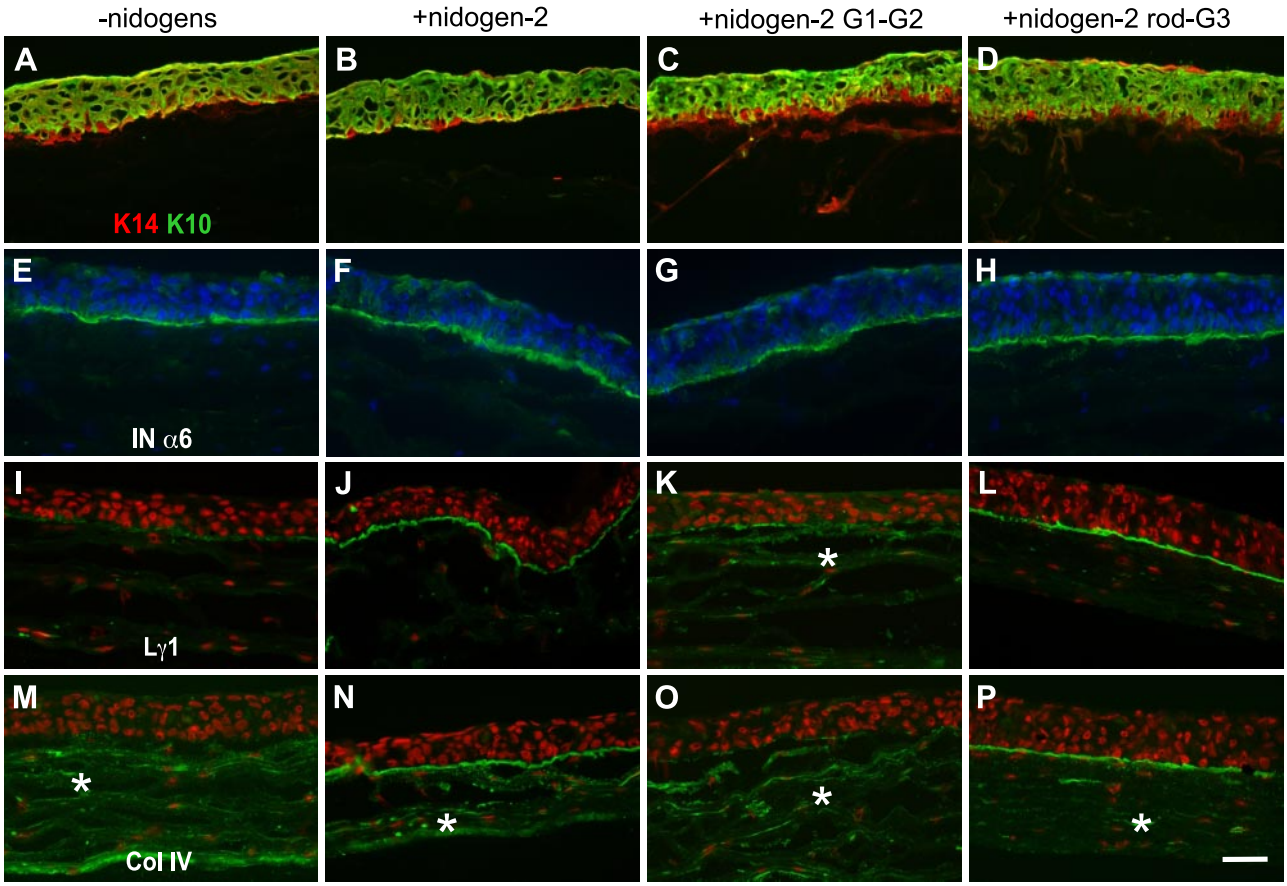

Figure 3. Epithelial organization and deposition of BM components in HaCaT cell/fibroblast 3D cocultures. Images show immunofluorescence stainings of cryosections from cocultures with nidogen-deficient mouse fibroblasts without (*A, E, I, M*) and with addition of either 3 μg/ml recombinant nidogen-2 (*B, F, J, N*), nidogen-2 G1–G2 (*C, G, K, O*), or nidogen-2 rod–G3 (*D, H, L, P*) to the culture medium. Whether the staining marked by asterisks represents collagen IV stretches or autofluorescence from collagen fibers is unclear (*K, M–P*). Supplementation was performed throughout the cultivation time of 12 d. Epithelial differentiation and organization were assessed by immunofluorescence staining with antibodies raised against the basal keratin 14 (K14; *A–D*), the suprabasal keratin 10 (K10; *A–D*), and the integrin α6 chain (IN α6; *E–H*). Deposition of BM components was analyzed with antibodies directed against the laminin γ1 chain (Lγ1; *I–L*), detecting laminin-511, and collagen IV (Col IV; *M–P*). Secondary antibodies conjugated to Alexa 488 (green) were used to detect the integrin α6 chain, the laminin γ1 chain, collagen IV, and keratin 10, and Alexa 594 (red) was used to detect keratin 14. Propidium iodide (red) or DAPI (blue) was used to stain nuclei. A representative set of cocultures out of 3 independently performed experiments is shown. Scale bar = 40 μm.

domain could drive deposition of the laminin γ1 chain and collagen IV at the junctional interface (Fig. 3*J, L, N, P*). As shown for nidogen-1, the nidogen-2 domain G1–G2 also could not restore deposition of these components (Fig. 3*K, O*). However, under all conditions, stretches stained with collagen IV antibodies are visible (Fig. 3*M–P*). Whether these stretches represent collagen IV staining or autofluorescence from collagen fibers is unclear. Further, some weak focal staining for the laminin γ1 chain is seen in cultures supplemented with nidogen-1 and -2 fragments (Figs. 2*I–L* and 3*I–L*). Interestingly, only the nidogen fragments that are able to trigger BM deposition are found at the epidermal-collagen gel interface (Supplemental Fig. S1), indicating that in this coculture system ternary complex formation is a prerequisite for recruiting nidogens to BMs.

Laminin-332 staining, although dramatically reduced, was still detectable in varying intensities in the absence of active nidogen-1 and -2 fragments. However, strong continuous and linear laminin-332 staining was only seen in the presence of nidogen-1, nidogen-2, and the nidogen-2 rod–G3 domain (Supplemental Fig. S2). Thus, the necessary clustering of hemidesmosomal components seems to require appropriate condensation of matrix molecules facilitated by nidogen. In contrast to laminin-332, which is only expressed by keratinocytes and only found in BMs, perlecan is secreted by both fibroblasts and keratinocytes and also found outside of BMs. In mouse skin, it is detected in the junctional BM and also in high amounts below the BM in the upper dermis (31). Accordingly, immunofluorescence analysis using perlecan antibodies under the various culture conditions revealed broad staining throughout the collagen gel with a higher intensity close to the interface. Only with the full-length nidogen-1 and -2 and to a lesser extent with the G1–G2 domains of both nidogens, a continuous and linear deposition of perlecan at the junctional interface was detected (Supplemental Fig. S2).

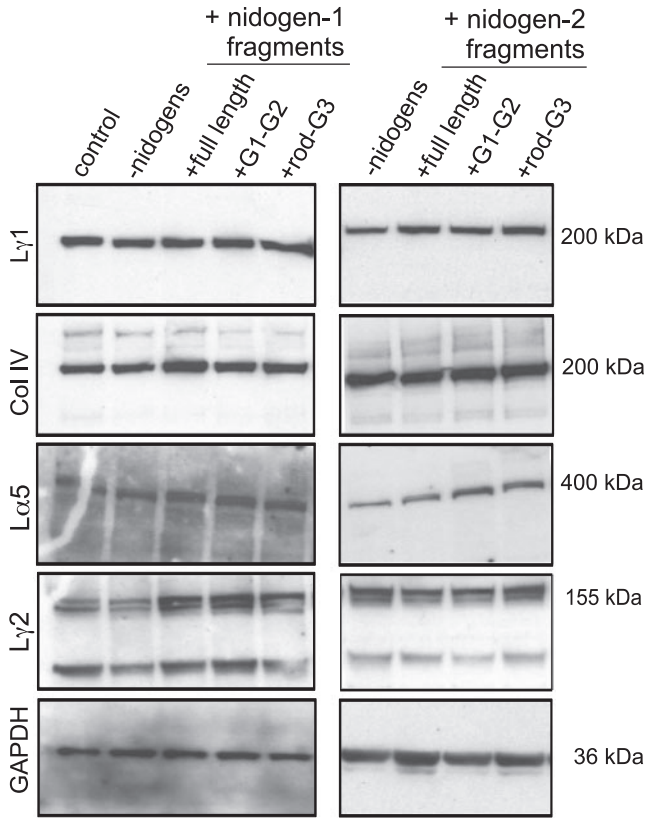

Figure 4. Western blot analysis of BM proteins in extracts from HaCaT cell/fibroblast 3D cocultures populated with nidogen-deficient fibroblasts with and without addition of recombinant nidogen fragments (12 d). Protein extracts from 3D cocultures treated with different nidogen-1 (left panel) or nidogen-2 (right panel) fragments were used. Fifty micrograms of total protein per lane was resolved on 4-12% SDS-polyacrylamide gels under reducing conditions. As a loading control, antibodies directed against GAPDH were applied. Control, protein extract from cocultures with nidogen-expressing fibroblasts. Molecular masses (kDa) of the proteins are indicated at right for both panels. BM components detected are the laminin γ1 chain (Lγ1), collagen IV (Col IV), the laminin α5 chain (Lα5), and the laminin γ2 (Lγ2) chain.

To determine the fate of these and other BM components in the different coculture combinations, protein extracts from the cocultures were analyzed by Western blotting (**Fig. 4**). Under all culture conditions, with or without nidogen fragments, comparable amounts of the laminin α5 and γ1 chains (laminin-511), the laminin γ2 chain (laminin-332), and collagen IV were detected. The partial processing of the laminin γ2 chain from a 155- to 105-kDa band (32) was also indistinguishable in all coculture combinations. This finding indicates substantially unaltered synthesis and processing of BM components independent of the culture conditions and the outcome.

Electron microscopy of cocultures supplemented with either nidogen-1 or nidogen-2 fragments supported the results obtained by indirect immunofluorescence (Figs. 2 and 3). Under all culture conditions in which simultaneous deposition of the laminin γ1 chain and collagen IV was observed, an ultrastructurally defined BM zone with developing and mature hemidesmosomes had been formed (**Fig. 5**). Collectively, supplementation with nidogen-1 (Fig. 5*C*) or nidogen-2 (Fig. 5*D*), with the domain G2–G3 of both nidogens (Fig. 5*E, F*, immunofluorescence stainings not shown), and with nidogen-2 rod–G3 (Fig. 5*J*) resulted in BM structures similar to those seen in cocultures with nidogen-expressing fibroblasts (Fig. 5*A*). With nidogen-2 rod–G3 the hemidesmosomes and the attached BM appear less well-structured, suggesting a slightly slower assembly in the presence of this fragment. In contrast, in cocultures with nidogen-deficient fibroblasts (Fig. 5*B*) supplemented with either the G1–G2 domain of nidogen-1 or -2 (Fig. 5*G, H*) or the rod–G3

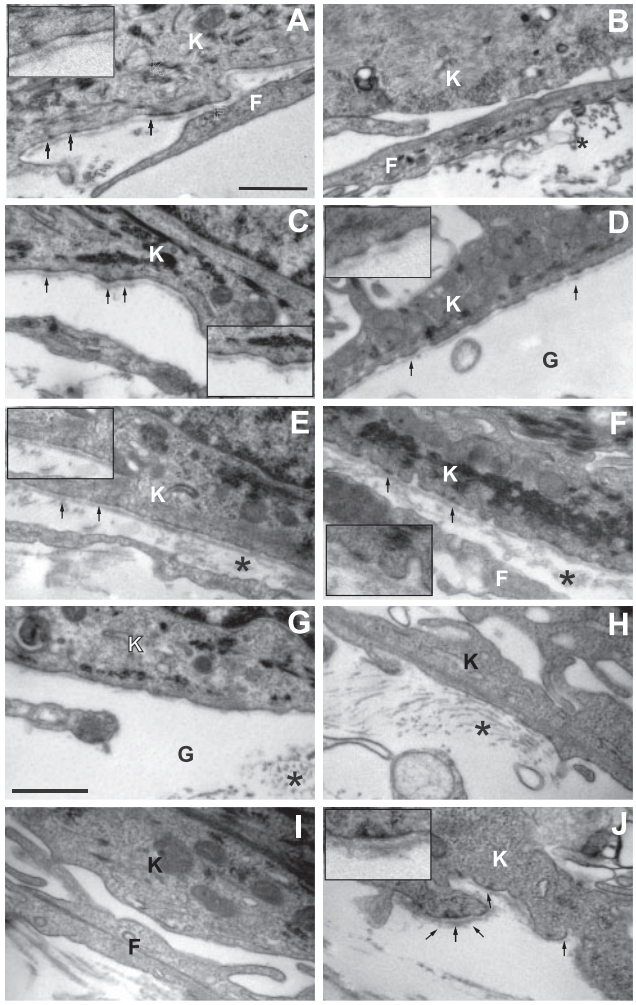

Figure 5. *A, B*) Electron micrographs of ultrathin sections of 3D cocultures composed of HaCaT cells and nidogen-expressing (*A*) and nidogen-deficient (*B*) murine fibroblasts. *C–J*) Three-dimensional cocultures with nidogen-deficient fibroblasts after incubation with nidogen-1 (*C*), nidogen-2 (*D*), nidogen-1 G2–G3 (*E*), nidogen-2 G2–G3 (*F*), nidogen-1 G1–G2 (*G*), nidogen-2 G1–G2 (*H*), nidogen-1 rod–G3 (*I*), and nidogen-2 rod–G3 (*J*). Asterisks mark collagen I fibrils. Arrows mark hemidesmosomes and the attached BM. Insets: 2-fold magnification. K, keratinocyte; F, fibroblast; G, collagen gel. Scale bar = 0.5 μm.

domain of nidogen-1 (Fig. 5*I*), no signs of BM assembly could be observed.

In summary, immunofluorescence and ultrastructural analysis demonstrated that nidogen-1 requires both the G2 and G3 domains to achieve deposition of BM components and BM assembly, whereas nidogen-2 requires only the G3 domain.

The G3 domain of nidogen-2 is able to mediate complex formation between laminin and collagen IV, whereas nidogen-1 needs both the G2 and the G3 domain

Previous studies have shown that nidogen-1 requires the G2 and G3 domains for ternary complex formation with collagen IV and laminin. The collagen IV binding activity has been localized to G2 and the laminin binding activity to G3 (9, 14). Interestingly, the results obtained in this study indicate that nidogen-2 can simultaneously bind collagen IV and laminin by its isolated G3 domain alone. To obtain independent support for this result, solid-phase binding assays were performed with collagen IV as the immobilized ligand. With the streptavidin-tagged short arm of the laminin γ1 chain as the soluble ligand, almost no binding to collagen IV was observed (**Fig. 6*A, B,*** ctrl). However, prior incubation of the laminin γ1 short arm with the different His-tagged nidogen-1 and -2 fragments to allow the formation of laminin-nidogen complexes increased the collagen IV binding significantly for the full-length nidogen-1 and -2, for the G2–G3 domain of both nidogens, and, most interestingly, for the rod–G3 domain of nidogen-2 (Fig. 6*A, B,* shaded bars). This observation demonstrates that the binding activities located in the G3 domain of nidogen-2 are sufficient to connect collagen IV to laminin, whereas nidogen-1 requires both the G2 and G3 domains. With the fragments G1-G2 of nidogen-1 and -2 and with the rod-G3

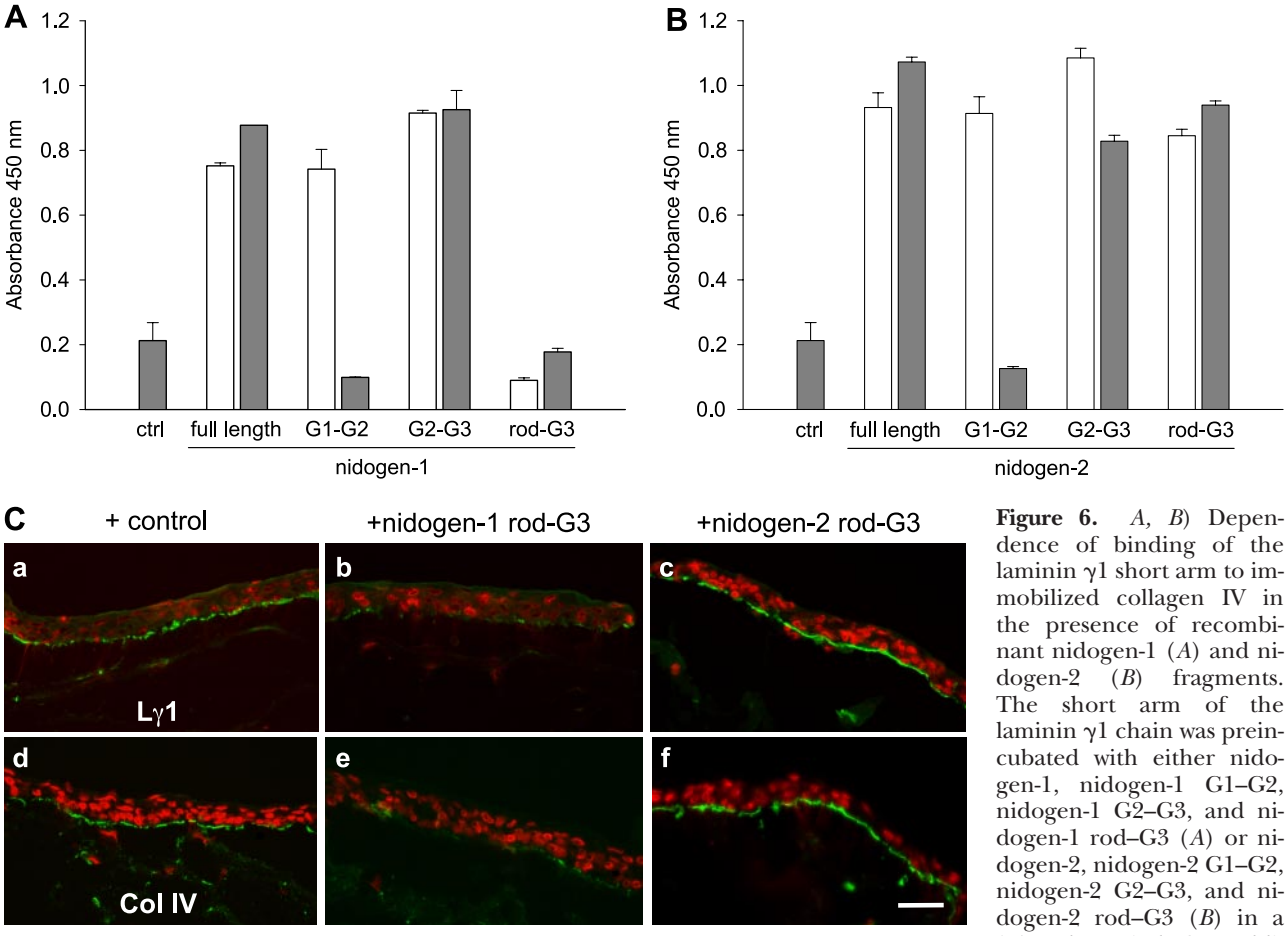

Figure 6. *A, B*) Dependence of binding of the laminin γ1 short arm to immobilized collagen IV in the presence of recombinant nidogen-1 (*A*) and nidogen-2 (*B*) fragments. The short arm of the laminin γ1 chain was preincubated with either nidogen-1, nidogen-1 G1–G2, nidogen-1 G2–G3, and nidogen-1 rod–G3 (*A*) or nidogen-2, nidogen-2 G1–G2, nidogen-2 G2–G3, and nidogen-2 rod–G3 (*B*) in a 2:1 molar ratio before addition to the collagen IV-coated 96-well plates. Detection of collagen IV binding by the different nidogen fragments was with antibodies directed against the His-tagged proteins (□). Ternary complex formation was determined using antibodies directed against the streptavidin tag of the laminin γ1 chain short arm (■). As a control, direct interaction of collagen IV with the laminin γ1 chain short arm was determined with antibodies directed against the streptavidin tag of the laminin fragment (■). Results are representative of 2 independent experiments, each performed in duplicate (mean±SE). *C*) Deposition of BM components in HaCaT 3D cocultures with nidogen-expressing fibroblasts without (control; *a, d*) and after addition of either 3 μg/ml recombinant nidogen-1 rod–G3 (*b, e*) or nidogen-2 rod–G3 (*c, f*) to the culture medium. Supplementation was performed throughout the cultivation time of 12 d. Indirect immunofluorescence staining was done on cryosections using antibodies directed against the laminin γ1 chain (Lγ1; *a–c*) and collagen IV (Col IV; *d–f*). Secondary antibodies conjugated to Alexa 488 (green) were used to detect the laminin γ1 chain and collagen IV. The nuclei were counterstained with propidium iodide (red). Scale bar = 40 μm.

domain of nidogen-1, no complex formation could be observed (Fig. 6*A, B*, shaded bars). However, the fragment G1–G2 of either nidogen binds to collagen IV as shown by antibodies directed against the His-tag, whereas in the presence of the laminin γ1 short arm, the G3 domain of nidogen-1 does not (Fig. 6*A, B*, open bars).

In summary, the solid-phase binding assays identified one collagen IV binding site in nidogen-2 located within the domain G2 and a second one located within G3. For nidogen-1, only one collagen IV- binding site, located in domain G2, could be detected. Moreover, only the nidogen-2 G3 domain showed laminin-collagen IV connecting activity.

We could show that connecting collagen IV and laminin is a crucial step for BM assembly in skin organotypic cocultures. To provide additional functional evidence, we performed competition experiments using cocultures populated with fibroblasts expressing both nidogen isoforms. In these cocultures laminins containing the γ1 chain and collagen IV are deposited at the epithelial-collagen gel interface (Fig. 6*Ca, d*). Supplementation of the cocultures with an excess of the nidogen-1 rod–G3 domain resulted in the loss of laminin from the junctional interface by competitively inhibiting the laminin interaction of the endogenous nidogen-1 and -2. As a consequence, collagen IV deposition was blocked (Fig. 6*Cb, e*). In contrast, addition of the nidogen-2 rod–G3 domain did not interfere with collagen IV and laminin deposition. It seems that the presence of this domain enhanced assembly of these proteins at the junctional interface (Fig. 6*Cc, f*). This is in agreement with previously published data, showing in nidogen-deficient cocultures accelerated BM assembly by immunofluorescence and ultrastructural analysis after addition of recombinant nidogen-1 or -2 compared with that cocultures with wild-type fibroblasts (29).

DISCUSSION

The skin organotypic coculture system used in this study provides an excellent tool to dissect processes, such as BM assembly, which require a 3D environment and the cross-talk between epithelial and mesenchymal cells. Using this system, we previously showed that BM assembly was completely prevented in the absence of nidogens and that supplementation by either recombinant nidogen-1 or nidogen-2 could restore the structures of the BM zone (29). Loss of nidogens affected the BM zone in a manner similar to that for inhibition of the nidogen-laminin interaction by a laminin γ1 chain fragment comprising the high-affinity nidogen binding site (29, 33). However, from these studies, it remained unclear whether other interactions than those involving the laminin γ1 chain are significant for BM restoration.

Interactions of nidogens with the γ1III4 module of the laminin γ1 chain, shared by most laminin isoforms, and collagen IV were previously shown to mediate formation of ternary complexes and were considered to reflect a major role of nidogens in organizing and stabilizing certain BMs (8, 9, 11, 34, 35). To determine whether the capacity of nidogens to connect laminin and collagen IV is a prerequisite for BM deposition in 3D cocultures, we dissected the two nidogens into fragments comprising different domains with potential binding activity. For nidogen-1, the laminin binding site has been mapped to the G3 domain and the collagen IV binding site to the G2 domain (9, 14, 36). In contrast, the binding sites for laminin and collagen IV within nidogen-2 have not yet been identified. We therefore tested the different recombinantly produced nidogen-1 and nidogen-2 fragments in solid-phase assays using the short arm of the laminin γ1 chain, which contains the γ1III4 nidogen binding module and collagen IV as immobilized ligands. Solid-phase assays using nidogen-1 and its fragments as soluble ligands revealed binding to the laminin γ1 chain short arm only by the full-length protein containing the G3 domain and by the G3 domain alone, thus confirming published results (9, 14). The G1–G2 domain showed no binding activity. In nidogen-2, the same domain, G3, could be identified as the binding site for the γ1III4 module. The affinity of nidogen-2 to this laminin fragment was approximately 1 order of magnitude lower and thus comparable to previously published data obtained with the laminin fragment P1 (8).

Collagen IV binding to nidogen-1 and its fragments was only observed with the fragment G1–G2 and the full-length protein. This finding is in agreement with published data, in which the collagen IV binding site was mapped to the G2 domain of nidogen-1 (9, 36). In contrast, in nidogen-2, two collagen IV binding sites were identified, one located in the domain G1–G2 and the second in G3. Interestingly, by surface plasmon resonance assays a second collagen IV binding site was also found in the nidogen-1 G3 domain (14). However, this binding site has never been detected in solid-phase binding assays (9, 36).

In summary, the binding studies with nidogen-1 confirmed the previously mapped laminin γ1 chain and collagen IV binding sites. Moreover, for the first time, binding sites for the laminin γ1 chain and collagen IV could be assigned to distinct nidogen-2 domains, namely G3 and G2/G3, respectively. These results also demonstrate that the recombinantly produced nidogen fragments are correctly folded and functionally active.

Immunofluorescence analysis of 3D cocultures supplemented with nidogen-1 and its fragments revealed deposition of the laminin γ1 chain (part of laminin-511) and collagen IV only with the full-length protein. Simultaneous deposition of laminin and collagen IV could not be detected with the domains G1–G2 and G3, indicating that both the G2 and G3 domains are required to drive deposition. This was further corroborated by electron microscopy showing an ultrastructurally defined BM zone with developing and mature

hemidesmosomes comparable to structures observed after addition of the full-length protein in cocultures supplemented with a nidogen-1 fragment comprising the G2 and G3 domains. For nidogen-2, the situation was different. In contrast to nidogen-1, the G3 domain of nidogen-2 alone was sufficient to trigger deposition of the laminin γ1 chain and collagen IV. The nidogen-2 G1–G2 fragment was unable to do so, as shown earlier for nidogen-1 G1–G2 (9, 14). Quantification of laminin γ1 and collagen IV staining intensities at the epidermal-collagen gel interface revealed that nidogen-1 and nidogen-2 are equally efficient in triggering deposition of these components (data not shown). This result is in good agreement with *in vivo* data showing ultrastructurally unaltered BMs in the absence of either nidogen-1 or nidogen-2 (7, 15).

Interestingly, although no deposition of BM components was observed with the nidogen fragment G1–G2, BM components such as the laminin α5, γ1, and γ2 chains could be detected by Western blot analysis in amounts comparable to those seen in cocultures with BM deposition. This finding indicates that the lack of BM deposition had no striking effect on synthesis or turnover of BM components and implies a profoundly altered distribution of these components, rendering them virtually undetectable at the epithelial-collagen gel interface by immunofluorescence. In support of this interpretation, immunoelectron microscopy has shown a very diffuse distribution of laminin-332 and collagen IV in experiments in which laminin deposition was blocked and also no major changes in synthesis and turnover of these components (33).

Ultrastructural analysis revealed a defined BM zone only under culture conditions in which simultaneous deposition of the laminin γ1 chain and collagen IV occurred, which demonstrates that the activity of nidogens to connect laminin and collagen IV is crucial for BM assembly in this culture system. This finding suggests that nidogens are catalyzing BM assembly by stabilizing the interactions between these components at the interface, thereby increasing the critical local concentration that may be required for BM formation.

This finding also suggests that the nidogen-1 domain G3, although possibly containing a collagen IV binding site (14), cannot simultaneously bind to laminin and collagen IV. This limitation is most likely due to steric constraints on the accessibility of the collagen IV binding site and indicates that the binding sites for laminin and collagen IV in the G3 domain of nidogen-1 are either spatially overlapping or identical. In contrast, the G3 domain of nidogen-2 was able to connect laminin and collagen IV, pointing to simultaneous accessibility of the two binding sites without steric hindrance. This finding was supported by solid-phase binding assays using collagen IV as the immobilized ligand. These assays revealed that only the full-length nidogen-1 and -2, the domains G2–G3 of both nidogens and, most importantly, the nidogen-2 rod–G3 domain could mediate complex formation between collagen IV and the soluble ligand, the laminin γ1 chain short arm. Ternary complex formation could not be detected with the nidogen-1 rod–G3 domain alone. In line with this, supplementation of nidogen-expressing cocultures with an excess of the nidogen-1 rod-G3 domain resulted in inhibition of BM deposition. The nidogen-2 rod–G3 domain, however, did not interfere with deposition of laminin and collagen IV, thus reaffirming the different binding behavior of the G3 domains of nidogen-1 and -2.

The difference in binding activities of the nidogen-1 and nidogen-2 G3 domains is surprising because these domains show a sequence homology of ~50% and a comparable modular composition (10). The two G3 domains show a highly conserved structure formed from 6 LDL receptor (LDLR) YWTD modules, which, as in LDLR itself, fold into a symmetrical 6-bladed β-propeller (37, 38). In the G3 domain of nidogen-1, an additional C-terminal epidermal growth factor (EGF)-like module is present. However, X-ray crystallography demonstrated that the β-propeller is sufficient to form a complex with the laminin γ1III4 module (38). The C-terminal EGF-like module is also found in invertebrates, which have only a single nidogen gene, suggesting a closer common ancestry to the vertebrate nidogen-1 (10, 39). Hence, nidogen-2 appears to have evolved from the vertebrate nidogen-1, retaining structural and functional similarities. However, changes in sequence may have caused alterations of binding affinities and accessibility of binding sites. In support of this assumption, the 3D structure of the complex revealed that the amino acid residues in the β-propeller of the G3 domain contacting the γ1III4 module are highly conserved between nidogen-1 and -2. In contrast, the binding surface contacting the γ1III3 module, an interaction that is insufficient for binding but augments affinity, is less well conserved (37, 38), which may explain the lower affinity of nidogen-2 for the γ1III4 module. Taken together with these observations, our results indicate that sequence changes in evolution have caused the differences in accessibility of binding sites in the G3 domains of the two nidogens and would also change the binding options of the two proteins. In contrast to nidogen-1, nidogen-2 would be able to bind perlecan *via* its G2 domain, simultaneously with binding collagen IV *via* G3. For nidogen-1, this is not possible because collagen IV and perlecan compete for the same binding site in domain G2 (40, 41).

In summary, we showed that in the skin organotypic model system the capacity of either nidogen-1 or nidogen-2 to connect laminin and collagen IV is a prerequisite for BM assembly. Interestingly, the linking activity could be assigned to different domains in nidogen-1 and nidogen-2, which in turn allows for different binding options of the two nidogens. Different binding options for nidogen-1 and -2 have been also observed *in vivo*. We showed that in mouse skin integration of nidogen-1 into BMs is completely dependent on the presence of the high-affinity nidogen-binding module on the laminin γ1 and γ3 chains (19, 20). In contrast, nidogen-2 is retained within the junctional BM in the absence of this module, indicating alternative binding

options for nidogen-2. Coimmunprecipitation experiments with polyclonal nidogen-2 antibodies showed precipitation of laminin and perlecan in the absence of the nidogen-binding module, suggesting alternative binding sites or partners (unpublished data). Interestingly, in skin organotypic cocultures perlecan deficiency did not interfere with BM formation. However, epidermal morphogenesis was affected, indicating a functional role of perlecan within BMs (42). Although nidogen binding to integrins has been reported *in vitro* (6, 8, 10), these data strongly argue against a direct role for integrins or other cell surface receptors in recruiting nidogens to the BM.

These different binding options have no structural consequence because the dermo-epidermal BM in mice lacking the nidogen-binding module appears ultrastructurally normal. However, epidermal hyperproliferation did occur, suggesting functional changes that could not be compensated for by nidogen-2 (20). Functional changes have also been observed in skin wound repair in the absence of nidogen-1 (17), although deletion of either *NID* gene did not interfere with skin homeostasis and BM formation (7, 10, 15). In the absence of nidogen-1 normalization of wound tissue is affected, showing prolonged epidermal hyperproliferation and a delay in epidermal differentiation as well as alterations in laminin deposition and integrin β1 and β4 distribution. No such changes have been observed in the absence of nidogen-2 (17).

In summary, although the different binding options of nidogen-1 and -2 as shown *in vitro* and *in vivo* have no structural consequences, the phenotypical differences between nidogen-1- and nidogen-2-null mice in wound healing and nerve tissues indicate that they could be of biological relevance for BM functions. FJ

The authors thank Marion Reibetanz and Isabell Koxholt (Department of Dermatology) for excellent technical assistance. The authors thank all colleagues listed in Materials and Methods for providing antibodies, plasmids, and cells expressing recombinant proteins. This work was supported by the Deutsche Forschungsgemeinschaft through the SFB 829 at the University of Cologne (to R.N. and W.B.) and the Baden-Württemberg Stiftung: Adult Stem Cells (P-LS-ASII/35 to P.B.).

REFERENCES

1. Timpl, R., and Brown, J. C. (1996) Supramolecular assembly of basement membranes. *Bioessays* **18,** 123–132
2. Aumailley, M., and Rousselle, P. (1999) Laminins of the dermo-epidermal junction. *Matrix Biol.* **18,** 19–28
3. Miner, J. H., and Yurchenco, P. D. (2004) Laminin functions in tissue morphogenesis. *Annu. Rev. Cell Dev. Biol.* **20,** 255–284
4. Smyth, N., Vatansever, H. S., Murray, P., Meyer, M., Frie, C., Paulsson, M., and Edgar, D. (1999) Absence of basement membranes after targeting the LAMC1 gene results in embryonic lethality due to failure of endoderm differentiation. *J. Cell Biol.* **144,** 151–160
5. Poschl, E., Schlotzer-Schrehardt, U., Brachvogel, B., Saito, K., Ninomiya, Y., and Mayer, U. (2004) Collagen IV is essential for basement membrane stability but dispensable for initiation of its assembly during early development. *Development* **131,** 1619–1628
6. Kohfeldt, E., Sasaki, T., Gohring, W., and Timpl, R. (1998) Nidogen-2: a new basement membrane protein with diverse binding properties. *J. Mol. Biol.* **282,** 99–109
7. Murshed, M., Smyth, N., Miosge, N., Karolat, J., Krieg, T., Paulsson, M., and Nischt, R. (2000) The absence of nidogen 1 does not affect murine basement membrane formation. *Mol. Cell. Biol.* **20,** 7007–7012
8. Salmivirta, K., Talts, J. F., Olsson, M., Sasaki, T., Timpl, R., and Ekblom, P. (2002) Binding of mouse nidogen-2 to basement membrane components and cells and its expression in embryonic and adult tissues suggest complementary functions of the two nidogens. *Exp. Cell Res.* **279,** 188–201
9. Fox, J. W., Mayer, U., Nischt, R., Aumailley, M., Reinhardt, D., Wiedemann, H., Mann, K., Timpl, R., Krieg, T., and Engel, J. (1991) Recombinant nidogen consists of three globular domains and mediates binding of laminin to collagen type IV. *EMBO J.* **10,** 3137–3146
10. Ho, M. S., Bose, K., Mokkapati, S., Nischt, R., and Smyth, N. (2008) Nidogens—extracellular matrix linker molecules. *Microsc. Res. Tech.* **71,** 387–395
11. Aumailley, M., Battaglia, C., Mayer, U., Reinhardt, D., Nischt, R., Timpl, R., and Fox, J. W. (1993) Nidogen mediates the formation of ternary complexes of basement membrane components. *Kidney Int.* **43,** 7–12
12. Mayer, U., Nischt, R., Poschl, E., Mann, K., Fukuda, K., Gerl, M., Yamada, Y., and Timpl, R. (1993) A single EGF-like motif of laminin is responsible for high affinity nidogen binding. *EMBO J.* **12,** 1879–1885
13. Poschl, E., Mayer, U., Stetefeld, J., Baumgartner, R., Holak, T. A., Huber, R., and Timpl, R. (1996) Site-directed mutagenesis and structural interpretation of the nidogen binding site of the laminin γ1 chain. *EMBO J.* **15,** 5154–5159
14. Ries, A., Gohring, W., Fox, J. W., Timpl, R., and Sasaki, T. (2001) Recombinant domains of mouse nidogen-1 and their binding to basement membrane proteins and monoclonal antibodies. *Eur. J. Biochem.* **268,** 5119–5128
15. Schymeinsky, J., Nedbal, S., Miosge, N., Poschl, E., Rao, C., Beier, D. R., Skarnes, W. C., Timpl, R., and Bader, B. L. (2002) Gene structure and functional analysis of the mouse nidogen-2 gene: nidogen-2 is not essential for basement membrane formation in mice. *Mol. Cell. Biol.* **22,** 6820–6830
16. Bader, B. L., Smyth, N., Nedbal, S., Miosge, N., Baranowsky, A., Mokkapati, S., Murshed, M., and Nischt, R. (2005) Compound genetic ablation of nidogen 1 and 2 causes basement membrane defects and perinatal lethality in mice. *Mol. Cell. Biol.* **25,** 6846–6856
17. Baranowsky, A., Mokkapati, S., Bechtel, M., Krugel, J., Miosge, N., Wickenhauser, C., Smyth, N., and Nischt, R. (2010) Impaired wound healing in mice lacking the basement membrane protein nidogen 1. *Matrix Biol.* **29,** 15–21
18. Vasudevan, A., Ho, M. S., Weiergraber, M., Nischt, R., Schneider, T., Lie, A., Smyth, N., and Kohling, R. (2010) Basement membrane protein nidogen-1 shapes hippocampal synaptic plasticity and excitability. *Hippocampus* **20,** 608–620
19. Willem, M., Miosge, N., Halfter, W., Smyth, N., Jannetti, I., Burghart, E., Timpl, R., and Mayer, U. (2002) Specific ablation of the nidogen-binding site in the laminin gamma1 chain interferes with kidney and lung development. *Development* **129,** 2711–2722
20. Mokkapati, S., Fleger-Weckmann, A., Bechtel, M., Koch, M., Breitkreutz, D., Mayer, U., Smyth, N., and Nischt, R. (2011) Basement membrane deposition of nidogen 1 but not nidogen 2 requires the nidogen binding module of the laminin gamma1 chain. *J. Biol. Chem.* **286,** 1911–1918
21. Limat, A., Stockhammer, E., Breitkreutz, D., Schaffner, T., Egelrud, T., Salomon, D., Fusenig, N. E., Braathen, L. R., and Hunziker, T. (1996) Endogeneously regulated site-specific differentiation of human palmar skin keratinocytes in organotypic cocultures and in nude mouse transplants. *Eur. J. Cell Biol.* **69,** 245–258
22. Stark, H. J., Baur, M., Breitkreutz, D., Mirancea, N., and Fusenig, N. E. (1999) Organotypic keratinocyte cocultures in defined medium with regular epidermal morphogenesis and differentiation. *J. Invest. Dermatol.* **112,** 681–691
23. Berthod, F., Germain, L., Li, H., Xu, W., Damour, O., and Auger, F. A. (2001) Collagen fibril network and elastic system

remodeling in a reconstructed skin transplanted on nude mice. *Matrix Biol.* **20,** 463–473
24. Li, A., Pouliot, N., Redvers, R., and Kaur, P. (2004) Extensive tissue-regenerative capacity of neonatal human keratinocyte stem cells and their progeny. *J. Clin. Invest.* **113,** 390–400
25. El Ghalbzouri, A., Jonkman, M. F., Dijkman, R., and Ponec, M. (2005) Basement membrane reconstruction in human skin equivalents is regulated by fibroblasts and/or exogenously activated keratinocytes. *J. Invest. Dermatol.* **124,** 79–86
26. Boukamp, P., Petrussevska, R. T., Breitkreutz, D., Hornung, J., Markham, A., and Fusenig, N. E. (1988) Normal keratinization in a spontaneously immortalized aneuploid human keratinocyte cell line. *J. Cell Biol.* **106,** 761–771
27. Breitkreutz, D., Stark, H. J., Plein, P., Baur, M., and Fusenig, N. E. (1993) Differential modulation of epidermal keratinization in immortalized (HaCaT) and tumorigenic human skin keratinocytes (HaCaT-ras) by retinoic acid and extracellular Ca^{2+}. *Differentiation* **54,** 201–217
28. Breitkreutz, D., Schoop, V. M., Mirancea, N., Baur, M., Stark, H. J., and Fusenig, N. E. (1998) Epidermal differentiation and basement membrane formation by HaCaT cells in surface transplants. *Eur. J. Cell Biol.* **75,** 273–286
29. Nischt, R., Schmidt, C., Mirancea, N., Baranowsky, A., Mokkapati, S., Smyth, N., Woenne, E. C., Stark, H. J., Boukamp, P., and Breitkreutz, D. (2007) Lack of nidogen-1 and -2 prevents basement membrane assembly in skin-organotypic coculture. *J. Invest. Dermatol.* **127,** 545–554
30. Koch, M., Veit, G., Stricker, S., Bhatt, P., Kutsch, S., Zhou, P., Reinders, E., Hahn, R. A., Song, R., Burgeson, R. E., Gerecke, D. R., Mundlos, S., and Gordon, M. K. (2006) Expression of type XXIII collagen mRNA and protein. *J. Biol. Chem.* **281,** 21546–21557
31. Mokkapati, S., Baranowsky, A., Mirancea, N., Smyth, N., Breitkreutz, D., and Nischt, R. (2008) Basement membranes are differently affected by lack of nidogen 1 and 2. *J. Invest. Dermatol.* **128,** 2259–2267
32. Aumailley, M., El Khal, A., Knoss, N., and Tunggal, L. (2003) Laminin 5 processing and its integration into the ECM. *Matrix Biol.* **22,** 49–54
33. Breitkreutz, D., Mirancea, N., Schmidt, C., Beck, R., Werner, U., Stark, H. J., Gerl, M., and Fusenig, N. E. (2004) Inhibition of basement membrane formation by a nidogen-binding laminin γ1 fragment in human skin-organotypic cocultures. *J. Cell Sci.* **117,** 2611–2622
34. Ekblom, P., Ekblom, M., Fecker, L., Klein, G., Zhang, H. Y., Kadoya, J., Chu, M. L., Mayer, U., and Timpl, R. (1994) Role of mesenchymal nidogen for epithelial morphogenesis in vitro. *Development* **120,** 2003–2014
35. Kadoya, Y., Salmivirtam, K., Talts, J. F., Kadoya, K., Mayer, U., Timpl, R., and Ekblom, P. (1997) Importance of nidogen binding to laminin γ1 for branching epithelial morphogenesis of the submandibular gland. *Development* **124,** 683–691
36. Reinhardt, D., Mann, K., Nischt, R., Fox, J.W,, Chu, M. L., Krieg, T., and Timpl, R. (1993) Mapping of nidogen binding sites for collagen type IV, heparan sulfate proteoglycan, and zinc. *J. Biol. Chem.* **1993,** 10881–10887
37. Springer, T. A. (1998) An extracellular β-propeller module predicted in lipoprotein, epidermal growth factor precursors, and extracellular matrix proteins. *J. Mol. Biol.* **283,** 837–862
38. Takagi, J., Yang, Y., Liu, J. H., Wang, J. H., and Springer, T. A. (2003) Complex between nidogen and laminin fragments reveals a paradigmatic β-propeller interface. *Nature* **424,** 969–974
39. Nakae, H., Sugano, M., Ishimori, Y., Endo, T., and Obinata, T. (1993) Ascidian entactin/nidogen: implication of evolution by shuffling two kinds of cysteine-rich motifs. *Eur. J. Biochem.* **213,** 11–19
40. Hopf, M., Gohring, W., Ries, A., Timpl, R., and Hohenester, E. (2001) Crystal structure and mutational analysis of a perlecan-binding fragment of nidogen-1. *Nat. Struct. Biol.* **8,** 634–640
41. Kvasankul, M., Hopf, M., Ries, A., Timpl, R., and Hohenester, E. (2001) Structural basis for the high-affinity interaction of nidogen-1 with immunoglobulin-like domain 3 of perlecan. *EMBO J.* **20,** 5342–5346
42. Sher, I., Zisman-Rosen, S., Elihau, L., Whitelock, J. M., Maas-Szabowski, N., Yamada, Y., Breitkruetz, D., Fusenig, N. E., Arikawa-Hirasawa, E., Iozzo, R. I., Bergmann, R., and Ron, D. (2006) Targeting perlecan in human keratinocytes reveals novel roles for perlecan in epidermal formation. *J. Biol. Chem.* **281,** 5178–5187

Received for publication October 4, 2011.
Accepted for publication May 8, 2012.

Different domains in nidogen-1 and nidogen-2 drive basement membrane formation in skin organotypic cocultures

Manuela Bechtel, Manuel V. Keller, Wilhelm Bloch, et al.

FASEB J 2012 26: 3637-3648 originally published online May 23, 2012
Access the most recent version at doi:10.1096/fj.11-194597